Study on the Thin-Film Solar Cell with Periodic Structure Using FDFD Method

Yuan Wei[a], Bo Wu[a], Zhixiang Huang[a,*], Xianliang Wu[a,b,*]
[a]Key Laboratory of Intelligent Computing and Signal Processing, Anhui University, Hefei 230039,China
[b]School of Electronic and Information Engineering, Hefei Normal University, Hefei 230061,China
*Email: zxhuang@ahu.edu.cn,xlwu@ahu.edu.cn

***Abstract*-The optical absorption properties of the thin-film solar cell (SC) is an important manifestation of its performance. Finite-difference frequency-domain (FDFD) method is employed to discretize the Maxwell's equations for the designed structure. The relationship between the absorbed power density with the design structure and the incident angle were deeply explored. Our numerical results can provide a reference for the design and optimization of thin film solar cells.**

***Keywords*-Finite-difference Frequency-Domain Method, Thin-Film Solar Cell, Periodic Structure**

I. INTRODUCTION

Since solar energy is renewable, clean energy. In recent years, the research of the solar cell [1] (SC) is also increasing attention. However, thin-film SC is one important part of it; while its energy conversion efficiency is low. So there are a lot of work to do with energy conversion efficiency and reducing costs. We design suitable structure of the SC, and then use FDFD method for its numerical processing. Also, the relationship between the absorption efficiency with structure and incident angle is analyzed.

In order to improve the absorption efficiency of SC, the surface plasmon effect is introduced. Surface plasmon resonances (SPRs) are collective oscillations of the free electrons that are confined to surfaces and interact strongly with light resulting in a polarization. SPRs usually occur at the interface between a dielectric with the positive dielectric constant ε_r^d and a metal with the negative dielectric constant ε_r^m, and SPRs only exist when they satisfy $\mathrm{Re}(-\varepsilon_r^m) > \varepsilon_r^d$ [2]. The light absorption of SC is strengthened by SPRs, by comparing the field distribution of the two design structures.

In order to describe the propagation and scattering of sunlight within the SC，Maxwell's equation should be strictly solved. The finite-difference time-domain (FDTD) [3] and the FDFD methods are usually used to discretize the Maxwell's equation. For noble metals (such as Ag and Au), the complex dielectric constants [4] have to be described by a large number of summation terms in Lorentz-Drude model [5] in FDTD method. While FDFD method [6,7] can use an experimentally tabulated dielectric constants of the dispersive materials directly. In addition, FDFD method has a unique advantage in processing periodic structure and oblique incidence. FDFD method is adopted here, and the hybrid absorbing boundary condition (ABC) is used to reduce the spurious numerical reflections due to the perfectly matched layer (PML) can't work very well under periodic boundary condition [8].

II. THEORETICAL AND NUMERICAL CALCULATION MODEL

A. Model and FDFD Algorithm

Two two-dimensional plasmonic thin-film amorphous silicon (A-Si) SC structures with periodic structure are depicted in Fig.1. Since the *s*-polarized incident light cannot excite the SPRs[5], we mainly consider the *p*-polarized light with the electromagnetic components of H_z, E_x, and E_y. And all the materials are assumed non-magnetic (μ_r=1).

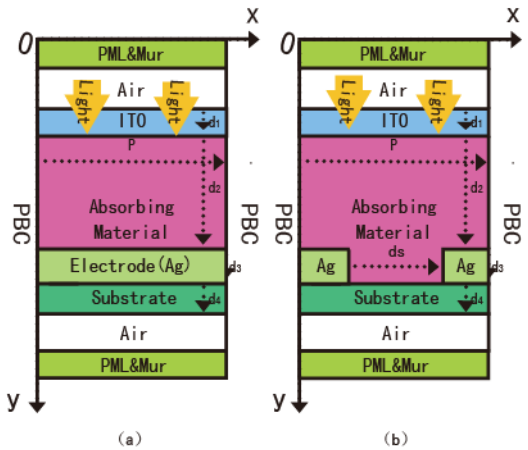

Figure 1. The unit cell of thin-film SC. (a) structure 1; and (b) structure 2,

As shown in Fig.1, the two structures include indium tin oxide (ITO), absorbing materials (A-Si), electrodes (Ag) and substrate with thickness d_1, d_2, d_3, d_4, respectively. The distance between two adjacent electrodes is d_s in the structure 2. The structure 2 is given to enhance the surface plasmon effect. The ABC is used with the PML and Mur absorbing boundary conditions, which is employed at the top and the bottom of the SC structure. The periodic boundary conditions (PBC) are imposed at the left and right sides of the unit cell.

For the isotropic and inhomogeneous media with the complex dielectric constant of $\varepsilon_r(x, y)$, the wave equation for the total field is given by [9]

$$\frac{\partial}{\partial x}\left(\frac{1}{\varepsilon_r(x,y)}\frac{\partial H_z^t}{\partial x}\right)+\frac{\partial}{\partial y}\left(\frac{1}{\varepsilon_r(x,y)}\frac{\partial H_z^t}{\partial y}\right)+k_0^2 H_z^t = 0 \qquad (1)$$

with k_0 is the wave number of free space. Using the second-order central differences, we have

$$\frac{\partial}{\partial x}\left(\frac{1}{\varepsilon_r(x,y)}\frac{\partial H_z^t}{\partial x}\right)=\frac{1}{\Delta x}\left(\frac{H_z^t(i+1,j)-H_z^t(i,j)}{\varepsilon_r(i+1/2,j)\Delta x}-\frac{H_z^t(i,j)-H_z^t(i-1,j)}{\varepsilon_r(i-1/2,j)\Delta x}\right)+O(\Delta x^2) \tag{2}$$

and Δx is the spatial step in x direction. The general treatment of the inhomogeneous material is shown in Fig. 2.

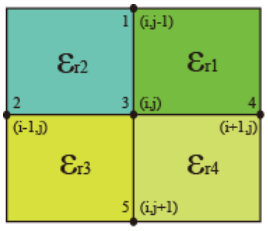

Figure 2. The inhomogeneous material treatment.

For the *p*-polarized incident light, the following averaging techniques is used,

$$\frac{1}{\varepsilon_r(i+1/2,j)}=\frac{1}{2}\left(\frac{1}{\varepsilon_{r1}}+\frac{1}{\varepsilon_{r4}}\right) \tag{3}$$

$$\frac{1}{\varepsilon_r(i-1/2,j)}=\frac{1}{2}\left(\frac{1}{\varepsilon_{r2}}+\frac{1}{\varepsilon_{r3}}\right) \tag{4}$$

Using the notation of $\Phi_1=H_z^t(i,j-1)$, $\Phi_2=H_z^t(i-1,j)$, $\Phi_3=H_z^t(i,j)$, $\Phi_4=H_z^t(i+1,j)$, and $\Phi_5=H_z^t(i,j+1)$, where the subscript 1,2,3,4 and 5 is the node as shown in Fig.2. (1) can be discretized into FDFD equation as

$$\sum_{m=1}^{5}c_m\Phi_m=0 \tag{5}$$

with

$$c_1=\frac{1}{2}\left(\frac{1}{\varepsilon_{r1}}+\frac{1}{\varepsilon_{r2}}\right)\cdot\frac{1}{\Delta y^2} \tag{6}$$

$$c_2=\frac{1}{2}\left(\frac{1}{\varepsilon_{r2}}+\frac{1}{\varepsilon_{r3}}\right)\cdot\frac{1}{\Delta x^2} \tag{7}$$

$$c_3=-\frac{1}{2}\left(\frac{1}{\varepsilon_{r1}}+\frac{1}{\varepsilon_{r2}}+\frac{1}{\varepsilon_{r3}}+\frac{1}{\varepsilon_{r4}}\right)\cdot\left(\frac{1}{\Delta x^2}+\frac{1}{\Delta y^2}\right)+k_0^2 \tag{8}$$

$$c_4=\frac{1}{2}\left(\frac{1}{\varepsilon_{r4}}+\frac{1}{\varepsilon_{r1}}\right)\cdot\frac{1}{\Delta x^2} \tag{9}$$

$$c_5=\frac{1}{2}\left(\frac{1}{\varepsilon_{r3}}+\frac{1}{\varepsilon_{r4}}\right)\cdot\frac{1}{\Delta y^2} \tag{10}$$

The total-field H_z^t can be calculated by solving (5), and the incident-field H_z^{inc} is known, so the scattered-field H_z^s is obtained by $H_z^t=H_z^{inc}+H_z^s$.

B. Boundary Conditions

As shown in Fig.1, the ABCs are used at the top and bottom respectively in order to reduce reflections. The complex coordinate PML [10] is applied as

$$\frac{\partial^2 H_z^s}{\partial x^2}+\frac{1}{s_y}\frac{\partial}{\partial y}\left(\frac{1}{s_y}\frac{\partial H_z^s}{\partial y}\right)+k_0^2H_z^s=0 \tag{11}$$

with

$$s_y=\begin{cases}1-j_0\dfrac{\sigma(y)}{\omega\varepsilon_0}, \text{in } PML\\ 1, \quad \text{else}\end{cases} \tag{12}$$

where ε_0 is the permittivity of free space, ω is the angular frequency of the incident light, and conductivity σ is employed by

$$\sigma(j)=\frac{C}{\Delta y}\left(\frac{j-1/2}{L}\right)^Q,\ j=1,2,...,8 \tag{13}$$

$$\sigma(j+1/2)=\frac{C}{\Delta y}\left(\frac{j}{L}\right)^Q,\ j=0,1,...,8 \tag{14}$$

where L is the layer number of PML, Q is the order of the polynomial, and C is a constant. The optimized parameters are chosen as L=8, Q=3.7, C=0.02. Using the second-order central differences, we have

$$\frac{1}{s_y}\frac{\partial}{\partial y}\left(\frac{1}{s_y}\frac{\partial H_z^s}{\partial y}\right)=\frac{1}{s_y(j)\cdot\Delta y}\left[\frac{H_z^s(i,j+1)-H_z^s(i,j)}{s_y(j+1/2)\cdot\Delta y}-\frac{H_z^s(i,j)-H_z^s(i,j-1)}{s_y(j-1/2)\cdot\Delta y}\right] \tag{15}$$

Taking the topmost lay of the structure y=0 as an example, the second-order Mur absorbing boundary conditions [11] can be employed by

$$\left[\frac{\partial}{\partial y}-j_0\left(k_0+\frac{1}{2k_0}\frac{\partial^2}{\partial x^2}\right)\right]H_z^s\Big|_{y=0}=0 \tag{16}$$

and its discretized form is given by

$$f_1H_z^s(i,j)+f_2H_z^s(i-1,j)+f_3H_z^s(i+1,j)+f_4H_z^s(i,j+1)=0 \tag{17}$$

with

$$f_1=2\exp(j_0k_0\Delta y)-2k_0^2\Delta x^2\exp(j_0k_0\Delta y)-2 \tag{18}$$

$$f_2=f_3=1-\exp(j_0k_0\Delta y) \tag{19}$$

$$f_4=2k_0^2\Delta x^2 \tag{20}$$

The periodic boundary conditions along the x direction can be described as

$$H_z^s(x+P,y)=H_z^s(x,y)\exp(-j_0k_0\cos\theta\cdot P) \tag{21}$$

$$H_z^s(x,y)=H_z^s(x+P,y)\exp(j_0k_0\cos\theta\cdot P) \tag{22}$$

with P is the periodic, and θ is the incident angle along x direction.

III. Numerical Results and Analysis

For the two-dimensional plasmonic thin-film SC with periodic structure as shown in Fig.1, the absorbing material is A-Si, the electrode is Ag, and the substrate is SiO2. The geometric parameters of the left structure are set as d_1=25nm, d_2=140nm, d_3=40nm, d_4=30nm, and P=200nm. Taking into account the consistency of the structure, the geometric

parameters of the right structure are set as d_1=25nm、d_2=120nm、d_3=40nm、d_4=30nm, P=200nm, and d_s=100nm. The y-directed incident field is the p-polarized plane wave with $H_z^{inc}(x,y)=\exp(-jk_0(x\cdot\cos\theta+y\cdot\sin\theta))$, the spatial step is set as Δx=Δy=0.5nm, θ is the incident angle. Here we chose θ equals 30º, 60º, and 90º, respectively.

Fig.3 shows the absorbed power density η for the two structures of A-Si when the incident angle is 90º. The formula is given by

$$\eta=\frac{\int_{Sa}\sigma_a|\mathbf{E}|^2\,ds}{\Delta Sa} \tag{23}$$

where ΔSa is the area of the A-Si, and σ_a=-$\omega\varepsilon_0$Im(ε_{ra}) is the conductivity of the A-Si. As shown in Fig.3, the absorbed power density of structure 2 is bigger than structure 1 at low-frequency portion (i.e. λ>660nm). The $|\mathrm{E}|^2$ of (23) will enhance since the generated of SPR, So the structure 2 shows stronger absorption than structure 1.

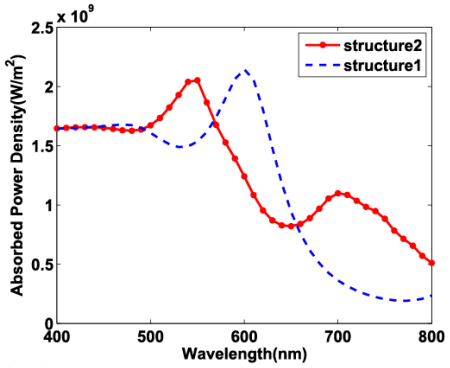

Figure 3. The absorbed power density by the A-Si for the two structures

The generalized reflection coefficient and transmission coefficients of the two structures are showed in Fig.4, the formula is employed as following

$$\begin{cases} R=\dfrac{\left|\dfrac{1}{P}\int_0^P H_z^s(x,y_r)\exp(jk_0x\cos\theta)dx\right|^2}{b^2} \\ T=\dfrac{\left|\dfrac{1}{P}\int_0^P H_z^t(x,y_t)\exp(jk_0x\cos\theta)dx\right|^2}{b^2} \end{cases} \tag{24}$$

where b is amplitude of the incident light. The absorption $A(\lambda)$ is introduced for comparison with the absorbed power density. It is defined as

$$A(\lambda)=1-R(\lambda)-T(\lambda) \tag{25}$$

Fig.4 (b) shows the absorption $A(\lambda)$, the trends of the absorption coincide with the trends of the absorbed power density, they all reflect the fact that the absorptions of structure 2 are strengthened at low-frequency portion due to the SPRs.

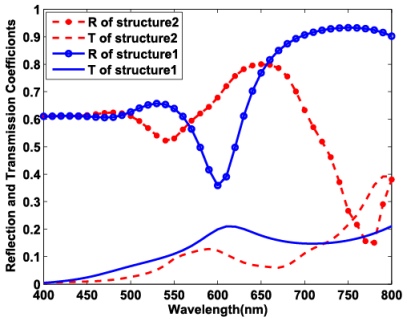

(a)

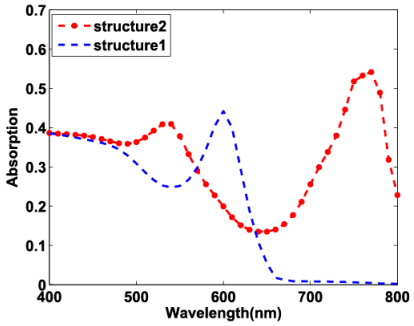

(b)

Figure 4. Spectrum results for the two structures. (a) The reflection and transmission coefficients; and (b) the absorption coefficients.

Fig.5 shows the total magnetic field H_z^t at λ=600nm, λ=650nm, λ=710nm, and λ=780nm, respectively. We can clearly see the enhancement of the total magnetic field at the interface of Ag layer and A-Si layer due to the SPRs.

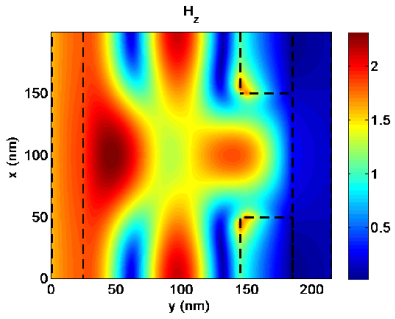

(a)

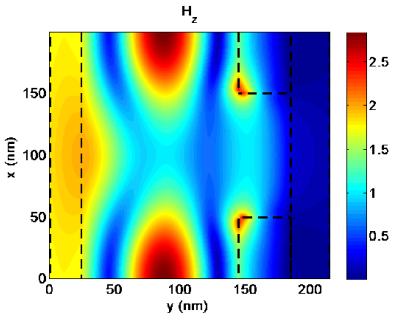

(b)

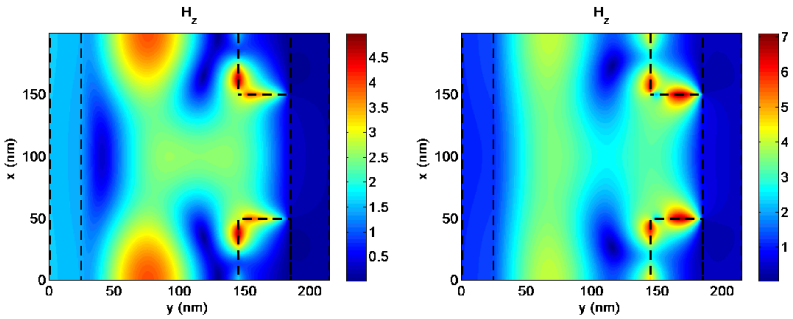

(c) (d)

Fig.5 The H_z^t field distribution for the structure 2 at different wavelengths. (a)λ=600nm; (b) λ=650nm; (c) λ=710nm; and (d) λ=780nm;

Enhancement factor $\kappa=\eta_2/\eta_1$ is employed to explanation why the enhancement of structure 2 is stronger than the enhancement of structure 1, where η_2 is the absorbed power density of structure 2, η_1 is the absorbed power density of structure 1. Next, we discuss the relationship between the incident angles with the enhancement factor as show in Fig.6. We can clearly see the enhancement factor is very large at low-frequency portion, which shows that structure 2 has better absorption properties due to the excited SPRs, and the enhancement factor increases with increasing of incident angle. It can increase to about 4.4 for the vertical incidence.

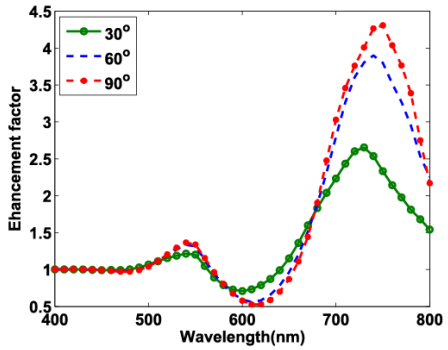

Figure 6. The relationship between enhancement factors with different incident angle.

IV. Conclusion

FDFD algorithm is used to numerical simulation of thin-film solar cell with periodic structure; the results show that the absorption of thin-film solar cell is related to the structure and the incident angle. Major impact on the structure is due to the SPRs which are excited at the interface of absorbing material and metal electrodes. In addition, the absorption in different incident angle is given due to FDFD algorithm can easily deal with the problem of oblique incidence. The results of our work can provide a theoretical basis and technical support for the design and optimization of the actual organic thin-film solar cells.

Acknowledgment

This work was supported by the National Natural Science Foundation of China under Grant (Nos. 60931002, 61101064, 51277001, 61201122), DFMEC (No.20123401110009) and NCET (NCET-12-0596) of China, Distinguished Natural Science Foundation (No.1108085J01), and Universities Natural Science Foundation of Anhui Province (No. KJ2011A002), and the 211 Project of Anhui University.

References

[1] J. Nelson, *The Physics of Solar Cells*, *London: Imperial College Press*, 2003.

[2] R. Zia, M. D. Selker, P. B. Catrysse, and M. L. Brongersma "Geometries and materials for subwavelength surface plasmon modes," *J. Opt. Soc. Am*, vol. 21, pp. 2442-2446, Dec. 2004.

[3] SUN Chen, LI Chuan hao, SHI Rui ying, SU Kai, GAO Hong tao, and DU Chun lei. "A Study of Influences of Metal Nanoparticles on Absorbing Efficiency of Organic Solar Cells," *Acta Photonica Sinica*, vol. 41, pp. 1335-1341, Nov. 2012.

[4] M. Qiu, and S. L. He, "A nonorthogonal finite-difference time-domain method for computing the band structure of a two-dimensional photonic crystal with dielectric and metallic inclusions," *J. Appl. Phys*, vol. 87, pp. 8268-8275, Jun. 2000.

[5] G. Veronis, and S. Fan, "Overview of Simulation Techniques for Plasmonic Devices," in Surface Plasmon Nanophotonics, M. L. Brongersma, and P. G. Kik, eds. *Springer, Dordrecht, The Netherlands*, 2007.

[6] Z. M. Zhu, and T. G. Brown, "Full-vectorial finite-difference analysis of microstructured optical fibers," *Opt. Express*, vol. 10, pp. 853-864, Aug. 2002.

[7] C. P. Yu, and H. C. Chang, "Compact finite-difference frequency-domain method for the analysis of twodimensional photonic crystals," *Opt. Express*, vol. 12, pp. 1397-1408, Apr. 2004.

[8] A. F. Oskooi, L. Zhang, Y. Avniel, and S. G. Johnson, "The failure of perfectly matched layers and towards their redemption by adiabatic absorbers," *Opt. Express*, vol. 16, pp. 11376-11392, Jul. 2008.

[9] W. C. Chew, *Waves and Fields in Inhomogenous Media*, *New York*, 1990.

[10] W. C. Chew, W. H. Weedon. "A 3-D perfectly matched medium from modified Maxwell's equations with stretched coordinates," *Microw. Opt. Technol. Lett*, vol. 7, pp. 599-604. Sep. 1994.

[11] G. Mur, "Absorbing boundary-conditions for the finite-difference approximation of the time-domain electromagnetic-field equations," *IEEE Trans. Electromagn. Compat*. Vol. 23, pp. 377-382, Nov.1981.